2003춘계학술발표회 논문집
한국원자력학회

Governing Factors to Delayed Hydride Cracking in Zr-2.5Nb Tubes

Young Suk Kim*, Sung Soo Kim, Yong Moo Cheong, In Sup Kim*
Korea Atomic Energy Research Institute, P.O. Box 105, Yusong, Daejon, 305-353, Korea
*Korea Advanced Institute of Science and Technology

Abstract

DHC tests have been carried out at different temperatures ranging from 100 to 280 ^{o}C on the compact tension specimens of Zr-2.5Nb pressure tubes with different yield strengths and the hydrogen concentration of 12 to 100 ppm. With the increasing supersaturated hydrogen concentration, DHC velocity (DHCV) of the Zr-2.5Nb pressure tubes has increased exponentially to a constant and its threshold stress intensity factor, K_{IH} also has decreased. Thus, DHCV and K_{IH} can be nicely described as a function of the supersaturated hydrogen concentration over the terminal solid solubility for dissolution (TSSD) independent of temperatures. Another factor to control DHCV is yield strength of the Zr-2.5Nb pressure tube: faster DHCV for the Zr-2.5Nb tubes with higher strength. By normalizing DHCV of the Zr-2.5Nb tubes by the solubility and diffusivity of hydrogen, DHCV is found to have a linear relation only with yield strength, irrespective of temperatures. Therefore, delayed hydride cracking of Zr-2.5Nb pressure tubes is governed by their tensile strength and a difference in the hydrogen concentration in solution between the crack tip and the bulk regions. A driving force for DHC is discussed from a view point of the concentration gradient and diffusivity of hydrogen.

1. Introduction

Since DHC is related to the movement of hydrogen from the bulk region to the crack tip under tensile stress, DHC velocity will be governed by diffusivity of hydrogen and the a concentration gradient of hydrogen between the crack tip and the bulk region even though the driving force for the gradient of hydrogen concentration is yet to be understood. It has been reported that yield strength [1] mainly affects DHC velocity among structural factors but the reason for this is not clearly understood. One suggested explanation was that the stress gradient between the notch tip and the bulk region would be steeper in the Zr-2.5Nb tube with higher yield strength, resulting in an enhanced diffusion of hydrogen and higher DHC velocity [1]. This suggestion was based on Dutton and Puls's DHC model that a main driving force for DHC is the stress gradient between the notch and the bulk region far away from it, leading hydrogen to dissolve from hydrides at the bulk, diffuse to the crack tip and precipitate there as hydrides [2,3]. However, since the yield strength of Zr-2.5Nb tubes are related to temperatures, textures and microstructures such as decomposition of the β-Zr phase, it is difficult to single out the effect of the yield strength on DHC velocity. Another thing is the driving force to cause the concentration gradient between the notch tip and the bulk region. Firstly, the effect of tensile stress on the solubility was suggested to be the driving force [4], which was confirmed to be wrong because the atomic volume of hydrogen in solution and that in the hydride is almost similar [5,6]. Then, an alternative hypothesis was proposed where tensile stress applied to the notch tip moves hydrogen in solution from the matrix to the notch tip with higher applied tensile stress [7,8]. As a result of that, this model predicted that the hydrogen concentration at the crack tip becomes larger by accompanying a decrease in the hydrogen concentration at the bulk region. If this concept is true, then the DHC velocity should have had a strong dependence on the applied tensile stress though the DHC velocity of the Zr-2.5Nb tubes, in reality, is constant irrespective of applied stress intensity factor [9]. In principle, the movement of hydrogen up against the concentration gradient as shown in Fig. 1 may be possible only under large tensile stress but this effect would be very small [10], leading to a very low or almost zero DHC velocity as in case where the test temperature is approached by heating up [11]. Consequently, we need another DHC model rather than the Puls' DHC model to explain the unresolved issues: the constant DHCV irrespective of applied stress intensity factor [9], a dependence of DHC velocity on hydrogen concentration [7,8] and so on.

One necessary step to reliably induce DHC in Zr-2.5Nb tubes is a thermal cycle where the Zr-2.5Nb

tube specimen is heated up to the peak temperatures before reaching the test temperatures. It is because DHC velocity depends on a difference between the peak temperature and the test temperature so that the peak temperature exceeds the test temperature by more than 40 ^{o}C [1]. At the peak temperature, the dissolved hydrogen concentration in the Zr-2.5Nb tube specimen reaches the terminal solid solubility for dissolution (TSSD) in accordance with the TSSD line given by Kearns [12] which is the same at the notch tip and the bulk region. However, when the Zr-2.5Nb tube specimen is cooled down to the test temperature, it maintains all the hydrogen in solution, leading to the supersaturation of hydrogen in solution both at the bulk region and the notch tip as was also suggested by Shek [1]. Since the extent of the supersaturation of hydrogen is determined by the temperature difference between the test temperature and the peak temperature, the temperature difference higher than 40 ^{o}C as reported by Shek [1] implies that there is a critical supersaturated concentration of hydrogen required to initiate DHC. As soon as tensile stress is applied on the Zr-2.5Nb tube specimen at the test temperature, it will trigger the nucleation of hydrides only at the notch tip [13], lowering the supersaturated hydrogen concentration to the equilibrium hydrogen concentration or TSSD corresponding to 250 ^{o}C. In contrast, the bulk region that is not subjected to tensile stress still maintains the supersaturated hydrogen concentration in solution, developing a difference in the hydrogen concentration between the crack tip and the bulk region. This is a driving force for DHC that lets hydrogen move to the crack tip from the bulk region continuously. From this view point, we think that the threshold stress intensity factor, K_{IH} is related to nucleation of hydrides at the crack tip, not to fracturing of hydrides. Since the nucleation of hydrides depends on the supersaturated hydrogen concentration and tensile stress, it can explain why the peak temperature shall increase to not less than 40 ^{o}C above the test temperature for the sufficient supersaturation of hydrogen.

The objective of this study is to investigate what are the governing factors to DHC and elucidate a driving force for DHC. To these ends, DHC velocity and K_{IH} of Zr-2.5Nb tubes were determined as a function of the hydrogen concentration and the effect of yield strength was elucidated through a normalization treatment of DHC velocity by the terminal solid solubility of hydrogen and the hydrogen diffusivity.

2. Experimental procedures

2.1. Materials

Two kinds of Zr-2.5Nb tubes with different microstructures as shown in Fig. 1 were used for evaluating the effect of yield strength on DHC velocity. Tube A with higher yield strength has elongated α-Zr grains and partially continuous β-Zr phase located between them whereas Tube B with lower yield strength has large equiaxed α-Zr grains and the transformed α-Zr grains of plate shape and fully discontinuous β-Zr phase located only between the transformed α-Zr grains. K_{IH} and DHC velocity were determined using 17 mm compact tension (CT) specimens taken from the Zr-2.5Nb tubes with electrolytically charged hydrogen as shown in Fig. 2. The hydrogen concentration of the CT specimens changed from 10 to 100 ppm by controlling their annealing temperatures after a thick hydride layer was formed on their surfaces. The details of the hydrogen charging procedures are reported elsewhere [14]. The real hydrogen content of the specimen was obtained by averaging 5 different values measured with a LECO RH 404 analyzer. A pre-fatigue crack of 1.7 mm was introduced using an Instron 8501 to have the ratio of the fatigue length and the CT specimen length or a_o/W equal to 0.5. The applied stress intensity factor was 12 MPa√m at the beginning stage of the pre-fatigue crack and was reduced to 10 MPa√m after the fatigue crack grew to 1.7 mm.

2.2. Delayed hydride cracking tests

The CT specimens were subjected to constant load in a creep machine while the initiation and growth of the crack were monitored by a dc potential drop method. Fig. 3 shows a typical thermal cycle to which the CT specimens were subjected during DHC tests. The CT specimens were heated to a peak temperature by 0.5-1 ^{o}C/min., held at the peak temperature for 1 h and cooled down to the test temperature followed by applying the load 30 minutes after reaching the test temperature. The peak temperature was set at 10 ^{o}C higher than the temperature of terminal solid solubility for dissolution (TSSD), dissolving all charged hydrogen completely. K_{IH} was determined in either the load increasing method or the load decreasing method [15]. For the load increasing method the initial applied load increased step-wise by 0.5 MPa√m from 4.5 MPa√m when the crack did not grow within 24 hours. K_{IH} was defined as the maximum stress intensity factor to grow the crack within 24 hours [15]. In the contrast, for the load decreasing method, the applied load decreased from 15 MPa√m step-wise by 0.5

MPa√m until the crack growth stopped. In the latter case, K_{IH} was defined as the minimum stress intensity factor to prevent the growth of the DHC crack within 24 hours [15]. More than two measured data were obtained at each test temperature for the reliability of the K_{IH} data. The crack length was determined on the fractured surface by dividing the area of the DHC crack calculated by an image analyzer by the width.

3. Results and discussion

3.1. Yield strength dependence

Fig. 4 shows the DHC velocity at 200 °C of the Zr-2.5Nb tubes with different yield strength. A nice correlation was obtained at the constant temperature between the DHC velocity and the yield strength of the Zr-2.5Nb tube: Tube A with higher yield strength had higher DHCV than Tube B with lower yield strength. However, when we plotted the DHC velocity determined at different temperatures as a function of the yield strength, no consistent relationship was found to exist between the yield strength and the DHC velocity as shown in Fig. 5. It is due to the temperature dependence of the DHC velocity. To eliminate any thermal effect on the DHC velocity arising from the solubility and diffusivity of hydrogen, we normalized DHC velocity with them and plotted the normalized DHC velocity as a function of the yield strength. Surprisingly, as shown in Fig. 6, we obtained a nice correlation of the normalized DHC velocity and the yield strength. It is to note that this DHC velocity dependence on the yield strength is also applicable to the irradiated Zr-2.5Nb tubes. Therefore, we conclude that the yield strength governs the DHC velocity of the Zr-2.5Nb tube. Furthermore, this leads to an understanding that the 3 to 5 times enhanced DHC velocity of the irradiated Zr-2.5Nb tubes compared to that of the unirradiated Zr-2.5Nb tubes [15] is attributed to the increased yield strength of the irradiated Zr-2.5Nb tube. Among the factors, or the solubility and diffusivity of hydrogen that governs the DHC velocity, it is the hydrogen diffusivity that the yield strength of the Zr-2.5Nb tube can have an influence on. It is because the hydrogen solubility is reported to have no change with the strength of the unirradiated Zr-2.5Nb tubes [16]. Since it has been theoretically demonstrated that hydrogen diffusion is enhanced by defects such as dislocations [17], higher DHCV with increasing yield strength is likely attributed to higher diffusivity of hydrogen in Zr-2.5Nb tubes. An empirical equation for the DHC velocity was derived as a function of yield strength as such [18]:

$$DHCV = 2032 C_H D_H \exp(0.00782\sigma_Y) = 2032 C_H D_H' \text{ [m/sec]} f(\Delta C). \quad (1)$$

where DHCV is the DHC velocity, C_H=hydrogen solubility=10.2exp(-35000/RT) [at.%], $D_H'=D_H\exp(0.00782\sigma_Y)=2.17\times10^{-7}\exp(-35100/RT+0.00782\sigma_Y)$, σ_Y=yield strength of the Zr-2.5Nb tubes and $f(\Delta C)$ is a function of the concentration gradient of hydrogen between the notch tip and the bulk region. In short, the effect of the yield strength is concluded to enhance hydrogen diffusion from the bulk region to the crack tip through defects such as dislocations.

3.2. Hydrogen concentration dependence

Figs. 7 and 8 show DHCV at 182 °C and K_{IH} at 280 °C of the Zr-2.5Nb tube as a function of total hydrogen concentration. With increasing hydrogen concentration, DHCV increased and got saturated to a constant (Fig. 7). Kim also reported that DHCV has no dependence on the hydrogen concentration when it is large enough [19]. In contrast, irrespective of the loading method, K_{IH} drastically decreased to a constant with the hydrogen concentration increasing as shown in Fig. 8. These results actually agree with the reported results by Shi [7] who also reported the dependence of the total hydrogen concentration on K_{IH} for which a clear-cut explanation is yet to be given.

Since we think that the extent of supersaturation of hydrogen in solution or ΔC is one of the governing factors to DHC, DHCV and K_{IH} shown in Figs. 7 and 8 were plotted again as a function of the supersaturated hydrogen concentration, ΔC as shown in Figs. 9 and 10, respectively. Here, ΔC is defined as the supersaturated hydrogen concentration in solution exceeding TSSD at the test temperature or C_0-TSSD, where C_0 is the total hydrogen concentration and TSSD is the terminal solid solubility of hydrogen. As expected, DHCV and K_{IH} could be represented well only as a function of ΔC. With increasing ΔC, DHCV increased exponentially and got saturated to a constant while K_{IH} decreased exponentially to a constant irrespective of the loading method. The critical ΔC value over which DHCV and K_{IH} got saturated to a constant was found to be approximately 30 ppm H, as shown in Figs. 9 and 10 while TSSP-TSSD corresponding to the test temperatures of 182 and 288 °C is 29 to 35 ppm H [12,20], respectively. Therefore, we can say that the critical ΔC value obtained from Figs. 9 and 10 agrees fairly

well with TSSP-TSSD. This fact proves that the maximum driving force, ΔC_{max} is TSSP-TSSD at the test temperature. When all K_{IH} data obtained at various temperatures were plotted only as a function of ΔC along with Shi's data[5], then K_{IH} can be nicely delineated only with ΔC independent of test temperatures as shown in Fig. 11. As expected, K_{IH} decreased exponentially with increasing ΔC and became constant when ΔC exceeded TSSP-TSSD. However, when ΔC approached 0, K_{IH} got infinitely large, leading to no occurrence of DHC.

The results shown in Figs. 9 to 11 demonstrate that DHC is governed by the supersaturated hydrogen concentration. When the specimen is heated up to the peak temperature, the hydrogen concentration dissolved in the Zr-2.5Nb tube specimen would follow up TSSD as shown in Fig. 13 (in accordance with the hydrogen solubility data given by Kearns [17]). During cooling-down to the test temperature, the equilibrium hydrogen concentration in solution would follow TSSP [18] as shown in Fig. 12 so that the crack tip and the bulk region maintain supersaturated hydrogen concentration in solution before the precipitation of hydrides. As soon as a tensile stress is applied to the crack tip, this will cause the nucleation of hydrides only at the crack tip [13], leading the supersaturated hydrogen concentration there to decrease to TSSD at the test temperature and developing a gradient of the hydrogen concentration between the crack tip and the bulk region. This nucleation process will go on until the supersaturated hydrogen concentration reaches TSSD, the equilibrium hydrogen concentration. Thus, the max attainable hydrogen concentration difference between the crack tip and the bulk region must be not more than TSSP-TSSD ($=\Delta C_{max}$) at the test temperatures, which is the driving force for DHC. Once the hydrides are nucleated, they seem to grow very fast because hydrogen moves almost instantaneously to the crack tip from the bulk region due to the developed hydrogen concentration gradient.

The nucleation process of hydrides will depend on applied tensile stress (or stress intensity factor) and the extent of supersaturation in the hydrogen concentration. Given the supersaturated hydrogen concentration at the crack tip, the applied stress intensity factor must be larger than the threshold stress intensity factor over which reoriented hydrides can nucleate only on the habit plane $\{10\bar{1}7\}$[21]. Thus, we think that K_{IH} is the threshold stress intensity factor to initiate the nucleation of reoriented hydrides at the crack tip, developing a hydrogen concentration gradient between the crack tip and the bulk regions. On the other hand, with a lesser degree of supersaturation of the hydrogen concentration in solution, the larger threshold stress intensity factor, K_{IH} is required to nucleate hydrides at the crack tip. This can explain an exponential increase in K_{IH} with the less saturated hydrogen concentration as shown in Figs. 10 and 11. When the supersaturated hydrogen concentration approached 0, then there is no way to nucleate hydrides even under enormously increased stress intensity factor, leading K_{IH} to approach the infinity. This leads to no growth of the DHC crack.

Since K_{IH} is related to the nucleation of hydrides from the crack tip with the supersaturated hydrogen concentration in solution, K_{IH} also would be affected by the test methods for determining K_{IH}. K_{IH} of the Zr-2.5Nb tube was determined at temperatures ranging from 160 to 280 ^{o}C using either the load-decreasing method or the load-decreasing method. The load-increasing method yielded larger K_{IH} over the investigated temperature range than the load-decreasing method as shown in Fig. 13. Under the load-decreasing method, the crack tip subjected to higher tensile stress will have the easy nucleation of hydrides, leading to lower K_{IH} as shown in Fig. 13. Conversely, under the load-increasing method, the hydrides will be more difficult to nucleate at the crack tip due to lower tensile stress, leading to higher K_{IH} as shown in Fig. 13. Therefore, the results shown in Fig. 13 provide supportive evidence that K_{IH} is the threshold stress intensity factor to initiate the nucleation of hydrides from the crack tip region with the supersaturated hydrogen concentration.

Once the supersaturated hydrogen concentration at the crack tip reaches TSSD under applied K_I larger than K_{IH}, then the hydrogen concentration at the crack tip will be in equilibrium and be maintained irrespective of applied stress intensity factor. This leads to developing the constant concentration gradient between the crack tip and the bulk region that is equal to TSSP-TSSD as shown in Fig. 12 irrespective of the total hydrogen concentration charged. This results in the constant DHC velocity independent of applied stress intensity factor. However, if the rate of cooling from the peak temperature to the test temperature changed, it would affect the TSSP line, leading to different ΔC and probably yield different DHCV with the cooling rate.

Therefore, we come to the conclusion that a driving force for DHC is ΔC or the concentration gradient in hydrogen in solution between the crack tip and the bulk region accompanied by the preferential nucleation of hydrides at the crack tip. One advantage of this new DHC model also can explain the effect of the way to approach the test temperature, heating-up or cooling-down. During cooling-down to

the test temperature from the peak temperature, the concentration gradient develops between the crack tip and the bulk regions as shown in Fig. 13. However, during heating up to the test temperature, the hydrogen concentration in solution would follow TSSD at 250 ^{o}C at the crack tip and the bulk regions, resulting in little gradient in the hydrogen concentration in solution between them even under applied tensile stress. This leads to little growth of the DHC crack [1,22].

The new DHC model suggests that no DHC occurs when the bulk hydrogen concentration is reduced to TSSD. There is experimental data [23] providing supportive evidence to this suggestion: when the critical temperature leading to a stop of the DHC growth was plotted as a function of the hydrogen concentration, the obtained slope agreed well with Kearns's hydrogen solubility curve. This experimental data demonstrated that no DHC occurs when the hydrogen concentration reached TSSD, proving that the above hypothesis is valid.

As a supplementary experiment to prove that ΔC governs DHC, we investigated the undercooling effect on DHCV when the test temperature, 250 ^{o}C was approached with the constant cooling rate from 310 ^{o}C. Here, the undercooling represents a temperature cycle where the CT specimen is cooled to temperatures lower than 250 ^{o}C and then heated up to 250 ^{o}C as shown in Fig. 14. When the amount of the undercooling varied from 0 to 40 ^{o}C as shown in Fig. 14, the hydrogen concentration in solution at the crack tip would become constant TSSD corresponding to the test temperature or 250 ^{o}C but the hydrogen concentration in solution at the bulk region would correspond to TSSP at the respective undercooled temperature. Thus, a difference in the hydrogen concentration between the crack tip and the bulk region, ΔC would vary from 0.7 to 22 ppm H, depending on the undercooled temperatures as shown in Table 1. The different amount of ΔC would affect DHCV.

Fig. 15 shows DHCV of the Zr-2.5Nb tube as a function of the degree of undercooling. With the increasing degree of undercooling, DHCV of the Zr-2.5Nb tube decreased. When DHCV was plotted as a function of ΔC, however, DHCV increased exponentially with increasing ΔC as expected as shown in Fig. 16. This exponential dependence of DHCV on ΔC as shown in Fig. 16 agreed exactly with the result shown in Fig. 9. This supplementary experiment provides other evidence that the driving force for DHC is ΔC or TSSP-TSSD at the test temperature. Therefore, DHCV and K_{IH} can be expressed as a function of ΔC as such: by putting the Eq. (1) together,

$$DHCV = A_1 C_H [\exp(\Delta C / \Delta C_{\max}) - 1] D_H \exp(A_3 \sigma_Y), \quad (2)$$

$$K_{IH} = A_2 \Delta G_m^* \exp[(\Delta C_{\max} - \Delta C) / \Delta C] f(a/w), \quad (3)$$

where A_1 and A_2 are constants, A_3 is constant ($MPa^{-}1$), C_H is hydrogen solubility [18], D_H is hydrogen diffusivity [18], ΔC is a difference in the hydrogen concentration between the crack tip and the bulk region at the test temperature, ΔC_{max} is a maximum attainable hydrogen concentration difference between the crack tip and the bulk region or TSSP-TSSD at the test temperature, f(a/w) is a geometric factor related to the notch shape and ΔG^*_m is a critical activation energy for the nucleation of 1 mol hydride that has a dependence on texture. It is to note that a missing point related to DHC is a discontinuous crack growth, which is beyond the scope of this study.

4. Conclusion

This study has investigated what are the goverining factors to delayed hydride cracking of Zr-2.5Nb tubes. Through a normalization of the DHC velocity by the solubility and diffusivity of hydrogen, we successfully singled out the effect of yield strength on the DHC velocity irrespecitve of test temperatures: the DHC velocity of the Zr-2.5Nb tubes increased exponentially with increasing yield strength. Based on a theoretical demonstration that hydrogen diffusion is enhanced by defects such as dislocations, higher DHCV with increasing yield strength is likely attributed to higher diffusivity of hydrogen in Zr-2.5Nb tubes. Therefore, we can suggest that the increased DHC velocity of the irradiated Zr-2.5Nb is attributed to an increase in their yield strength after neutron irradiation. Besides, it is the supersaturated hydrogen concentration in solution that governs the DHC velocity and threshold stress intensity factor, K_{IH} of the Zr-2.5Nb tubes: the larger the supersaturated hydrogen concentration becomes, the larger the DHC velocity and the lower the threshold stress intensity factor, K_{IH}. Thus, the K_{IH} is interpreted as the minium tensile stress to induce the nucleation of hydrides at the crack tip. Based on the results, we propose a new DHC model where the driving force for delayed hydride cracking of the Zr-2.5Nb tube arises from a difference in the hydrogen concentration between the crack tip and the bulk region

accompanied by the nucleation of hydrides only at the crack tip under applied tensile stress. A supplementary experiment was carried out where the supersaturated hydrogen concentration decreased with the increasing degree of undercooling, resulting in an exponential decrease in the DHC velocity of the Zr-2.5Nb tubes. This supplementary experiment provide supportive evidence that the proposed DHC model is feasible.

ACKNOWLEDGMENT

This work has been carried out under the Nuclear R&D Program supported by Ministry of Science and Technology (MOST), Korea.

References

[1] G.K. Shek and D.B. Graham, in Zirconium in the Nuclear Industry: Eighth International Symposium, ASTM STP 1023, L.F.P. Van Swam and C.M. Eucken, Eds, American Society for Testing Materials, Philadelphia, 1989, pp. 89-110.
[2] R. Dutton, K. Nuttal, M.P. Puls and L.A. Simpson, Metall. Trans., 1977, vol. 8A, pp. 1553-1562.
[3] M.P. Puls, L.A. Simpson and R. Dutton, in Fracture Problems and Solutions in the Energy Industry, L.A. Simpson, Ed., Pergamon Press, Oxford, 1982, pp. 13-25.
[4] R.L. Eadie and C.E. Coleman, Scripta Metall., 1989, vol. 23, pp. 1865-1870.
[5] G.J.C. Carpenter, J. Nucl. Mater., 1973, vol. 48, p. 264.
[6] S.R. MacEwen, C.E. Coleman, C.E. Ells and J. Faber, Acta Metall., 1985, vol. 33, pp. 753-757.
[7] S.Q. Shi and M.P. Puls, J. Nucl. Mater., 1994, vol. 218, pp. 30-36.
[8] S. Q. Shi, G.K. Shek and M.P. Puls, J. Nucl. Mater., 1995, vol. 218, pp. 189-201.
[9] C.E. Coleman and B. Cox, in Zirconium in the Nuclear Industry: Sixth International Symposium, ASTM STP 824, D.G. Franklin and R.B. Adamson, Eds, American Society for Testing Materials, Philadelphia, 1984, pp675-690.
[10] C.E. Ells and C.J. Simpson, in Hydrogen in Metals, I.M. Berstein and A.W. Thompson Eds, ASM Metal Park, 1974, pp. 345-366.
[11] J.F.R. Ambler, in Zirconium in the Nuclear Industry: Sixth International Symposium, ASTM STP 824, D.G. Franklin and R.B. Adamson, Eds, American Society for Testing Materials, Philadelphia, 1984, pp653-674.
[13] T.B. Flanagan and N.B. Mason, Scripta Metall., 1981, vol. 15, pp. 109-112.
[14] Y.S. Kim et al., KAERI/TR-1329/99, Korea Atomic Energy Research Institute, Daejeon, 1999.
[15] S. Sagat, C. E. Coleman, M. Griffiths and B. J. S. Wilkins, in Zirconium in the Nuclear Industry: Tenth International Symposium, ASTM STP 1245, A. M. Garde and E. R. Bradley, Eds., American Society for Testing and Materials, Philadelphia, 1994, pp. 35-61.
[16] A. McMinn, E.C. Darby and J.S. Schofield, in Zirconium in the Nuclear Industry: Twelfth International Symposium, ASTM STP 1354, G.P. Sabol and G.D. Moan, Eds., American Testing and Materials, West Consshohocken, PA, 2000, pp. 173-195.
[17] C.N. Park, J.Y. Lee, G.W. Hong, J. Mater. Sci. Letters, 1983, vol. 2, pp. 475-479.
[18] J.Y. Oh, I.S. Kim and Y.S. Kim, J. Nucl. Sci. &Tech., 2000, vol. 37, pp. 595-600
[19] Y.S. Kim, S.M. Seon, S.S. Kim. S.I. Kwun, J. Kor. Inst. Met. & Mater., 2000, vol. 38, pp. 35-43.
[12] J.J. Kearns, J. Nucl. Mater., 1967, vol. 22, pp. 292-303.
[20] Z.L. Pan, I.G. Rithie and M.P. Puls, J. Nucl. Mater., 1996, vol. 228, pp. pp. 227-237.
[21] Y.S. Kim, Y. Perlovich, M. Isaenkova, S.S. Kim and Y.M. Cheong, J. Nucl. Mater., 2001, vol. 297, pp. 292-302.
[22] Young Suk Kim, KAERI/TR-1137/98, Korea Atomic Energy Research Institute, Daejon, 1998.
[23] C.E. Coleman and J.F.R. Ambler, Scripta Metall., 1983, vol. 17, pp. 77-82.

Table 1. Hydrogen concentration difference between the crack tip and the bulk region with the degree of undercooling.

Undercooled Temperatures (^{o}C)	Amount of Undercooling (^{o}C)	$\Delta C=TSSP_{\text{undercooled Temp}}-TSSD_{\ 250\ oC}$ (ppm)
250	0	22
240	10	16
230	20	10
220	30	5
210	40	0.7

(a) 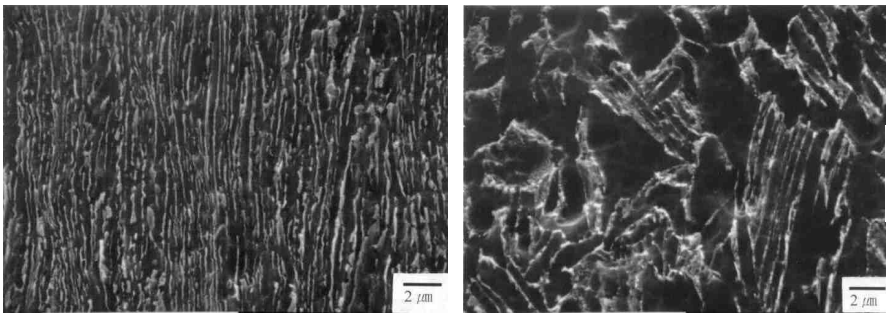 (b)

Fig. 1. Microstructures of the Zr-2.5Nb tubes: (a) Tube A and (b) Tube B..

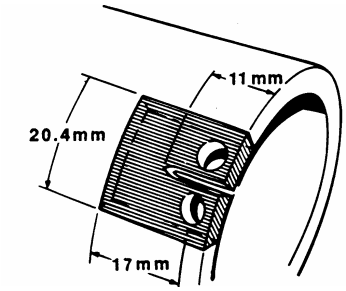

Fig. 2. Compact tension specimen used to determine the DHC velocity and the threshold stress intensity factor, K_{IH} of the Zr-2.5Nb tubes.

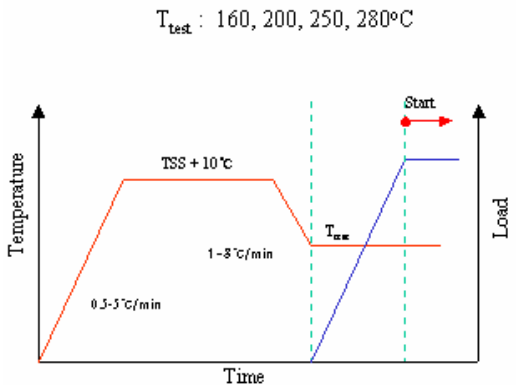

Fig. 3. Schematic diagram of a thermal cycle and loading schedule applied during DHC tests.

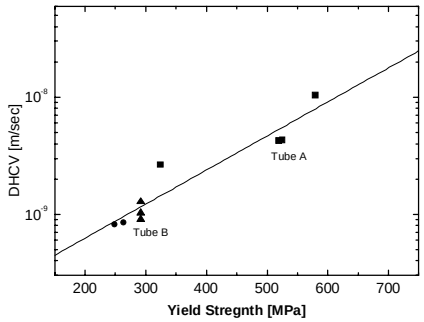

Fig. 4. DHC velocity at 200 °C of the Zr-2.5Nb tubes as a function of yield strength

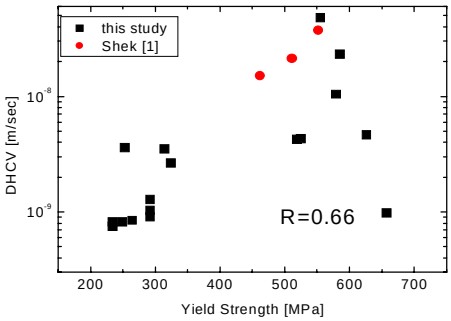

Fig. 5. DHC velocity at different temperatures of Zr-2.5tubes as a function of yield strength. No consistent relationship was found between DHC velocity and yield strength because of different temperatures

.

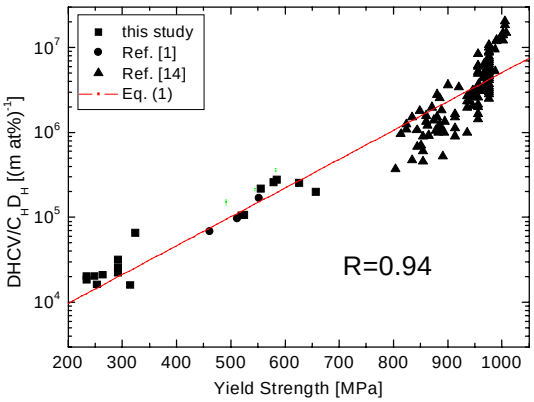

Fig. 6. A linear relationship of the normalized DHC velocity and yield strength independent of test temperatures.

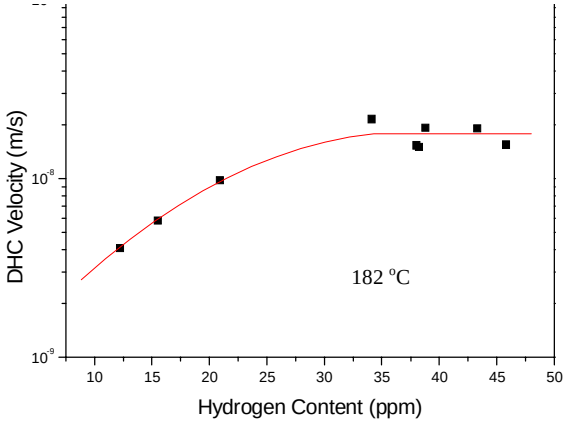

Fig. 7. Fig. 7. DHCV of the Zr-2.5Nb tube with the total hydrogen concentration at 182 °C.

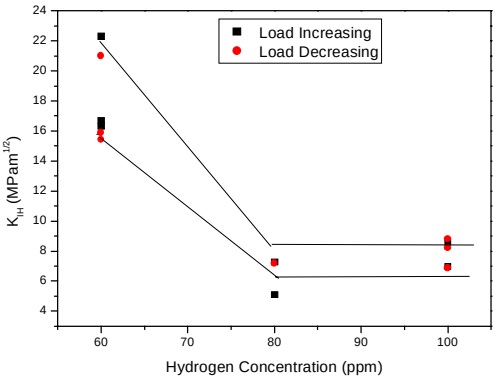

Fig. 8. Threshold stress intensity factor, K_{IH} of the Zr-2.5Nb with the total hydrogen concentration at 280 °C.

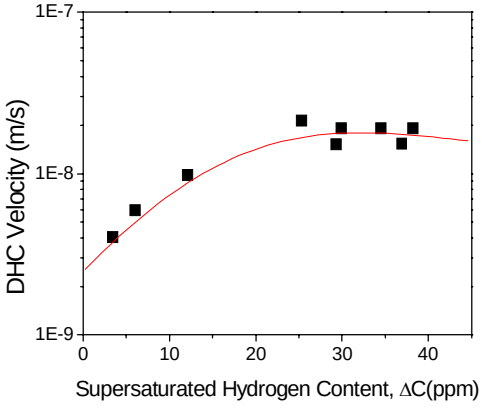

Fig. 9. DHCV of the Zr-2.5Nb tube with the superstaturated hydrogen concentration, ΔC at 180 °C.

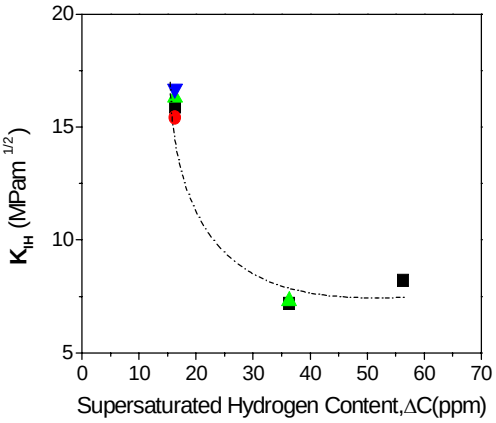

Fig. 10. Threshold stress intensity factor, K_{IH} of Zr-2.5Nb tube with the supersaturated hydrogen concentration, ΔC at 280 °C.

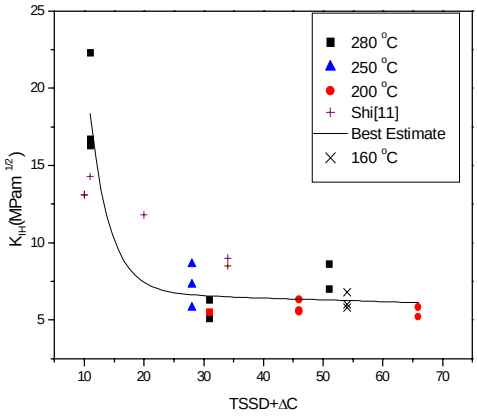

Fig. 11. KIH of Zr-2.5Nb tube as a function of the supersaturated hydrogen concentration, ΔC above TSSD at all temperatures

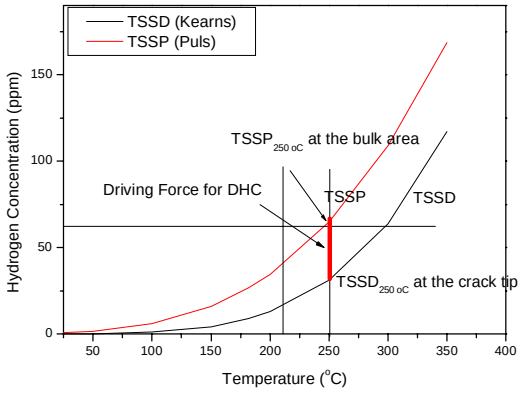

Fig. 12. The solvus lines of hydrogen during a thermal cycle to which the Zr-2.5Nb tubes is subjected during DHC tests. The driving force for DHC is a concentration gradient of hydrogen accompanied by the nucleation of hydrides at the crack tip under tensile stress: $TSSP_{\text{at the bulk area}} - TSSD_{\text{at the crack tip}}$ at the test temperatures.

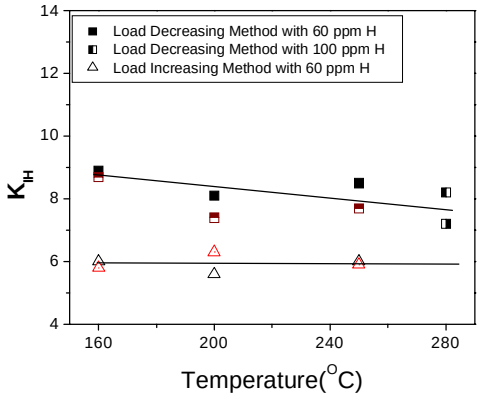

Fig. 13. Threshold stress intensity factor, K_{IH} of the Zr-2.5Nb tube with the loading method: load-decreasing or load-increasing methods.

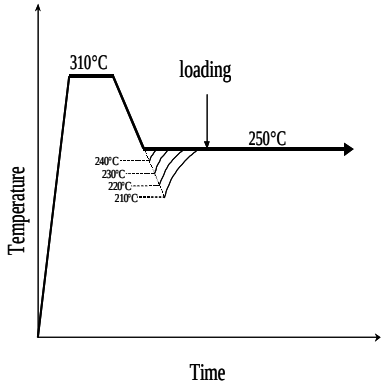

Fig. 14. Thermal maneuver to change the degree of undercooling from from 0 to 40 °C for the CT specimen with 60 ppm H.

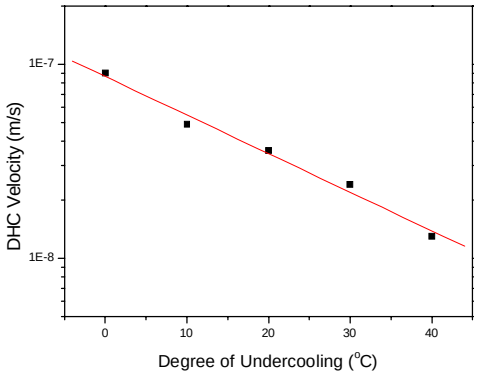

Fig. 15. DHCV at 250 °C of the Zr-2.5Nb tube with the undercooling.

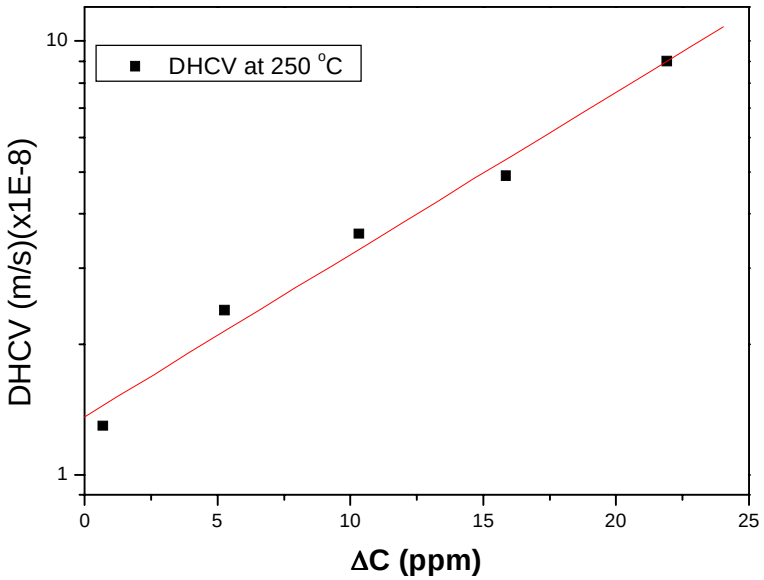

Fig. 16. DHCV at 250 °C of the Zr-2.5Nb tube with ΔC that was created by undercooling